Journal of Polymer Research (2018) 25: 24
https://doi.org/10.1007/s10965-017-1427-9

ORIGINAL PAPER

Double network epoxies with simultaneous high mechanical property and shape memory performance

Hanchao Liu[1] · Jiangbo Li[1] · Xiaoxiao Gao[1] · Bo Deng[1] · Guangsu Huang[1]

Received: 27 August 2017 / Accepted: 8 December 2017 / Published online: 18 December 2017

Abstract

Shape memory epoxy resins(SMEPs) with both high mechanical property and ideal shape memory performances were prepared by constructing double network structure through employing two kinds of curing agents with different reactivity. Results show that when the proportion of polyetheramine (D230) and diethyltoluenediamine (DETDA) are 40% and 60%, respectively, the tensile modulus, tensile strength and toughness of SMEPs are simultaneously enhanced compared with that of the samples cured with single curing agent. Meanwhile, shape memory properties still maintain at an ideal level when the proportion of D230 is 40%, while samples cured with pure DETDA show inferior shape memory property, especially at high tensile strain. DSC results show that the formation of network of sample cured with mixed curing agents can be divided into two steps, which may lead to a unique double network structure. Different network structures were characterized by DMA, TMA, and stress relaxation tests. Results show that physical network in the double network structure endows the epoxy resin with both enhanced strength and toughness while simultaneously maintained ideal shape memory performances.

Keywords Shape memory · Epoxy resin · Double network · Mechanical property

Introduction

Shape memory polymers (SMP) represent smart materials that can fix into a temporary shape after deformation and subsequently recover to their permanent shape upon external stimulation such as heat, pH, light, electricity, magnetic field or moisture [1–10]. The special shape memorizing ability of SMPs makes them an attractive and promising material meeting the requirements of different applications in various fields including textile materials, aerospace material, medical supplies, etc. [11–13].

Thermosets are an important class of SMP. In most cases, the reversible thermal transition of thermosets refers to the glass transition, above which polymer chain conformation changes and short range molecular mobility increases which provides a prerequisite for entropy changes. When the thermosets are heated above their glass transition temperature (T_g), a temporary shape can be got by applying an external stress. Then, the temporary deformation can be fixed by cooling below T_g, at which temperature the glass state is obtained that stores elastic energy and traps the entropy. When the stress is removed and the thermoset is heated again above T_g, a rapid recovery of the original shape is obtained as the entropy is released. Shape memory epoxy resin (SMEP) is an important family of shape memory thermosets. Because of the higher crosslinking density providing robust structure, versatile chemistry of curing and easy adjustability of preparing procedure, SMEPs are more suitable for application under harsh conditions than many other thermosets. Unfortunately, for SMEP, a contradiction between high mechanical properties and ideal shape memory performances is hard to avoid. According to L. Matějka, the shape fixity scales with the expression $(1 - G_r/G_s)$, where G_r and G_s are moduli below and above T_g, respectively [14]. However, high crosslinking density of SMEP usually leads to high modulus, especially G_r, which will cause an inferior shape fixity. What is worse, the low elongation of epoxy resin can also result in a poor recoverable deformation, which will severely restrict the application of the material. Generally, shape memory (SM) performances of SMEP can be improved by decreasing the

Electronic supplementary material The online version of this article (https://doi.org/10.1007/s10965-017-1427-9) contains supplementary material, which is available to authorized users.

✉ Guangsu Huang
guangsu-huang@hotmail.com

[1] College of Polymer Science and Engineering, State Key Laboratory of Polymer Material Engineering, Sichuan University, Chengdu 610065, China

crosslinking density of the crosslinking network, like tuning the proportion of the epoxy and the curing agent [15, 16]. However, this method will significantly decrease the stress and the modulus of the SMEP, which will restrict the application of the shape memory material [15, 16]. Polymer composites/nanocomposites, like polymer/nanoclay, polymer/fiber and polymer/nanotubes, are also constructed as SM systems to improve the SM performance of the polymer matrix [17, 18]. However, the difficulty in the design of cure schemes to guarantee a proper morphology of cured networks, and the poor processibility resulted from the high viscosity of the polymer-modifier blends furtherly restrained the application of these phase separated epoxy materials, such as fiber-reinforced composites and microelectronic applications [19].

Reinforcing of epoxy resin through design of intrinsic crosslinked networks will be an effective way to produce SMEPs with high mechanical properties. In the past few years, double network (DN) systems have been widely exploited to improve properties [20–22]. This double network structure often generates interesting stress–strain and thermal properties, which are highly correlated with shape memory performances. Thus, it is possible for double network epoxies to show different mechanical and shape memory performances. To the best of our knowledge, shape memory performances and comprehensive mechanical properties of epoxies with DN structure have not been reported. In this work, SMEPs with double network structure were prepared and mechanical and shape memory performances were studied. It was found that the construction of the double network structure can not only successfully improve the mechanical properties of the SMEPs, but also maintain an ideal shape memory performance and keep good thermal property, which may provide a new perspective for preparing SMEPs with high mechanical performance.

Materials and methods

Materials

DGEBF, with an epoxy equivalent weight of 170 g (equiv)$^{-1}$, was purchased from Luohe Chemistry Co. Ltd., China. Curing agent, diethyltoluenediamine (DETDA), was purchased from Puyang Huicheng Electronic Material Co. Ltd., China. Poly(propylene glycol) bis (2-aminopropyl)ether (Jeffamine D230) and 2-ethyl-4-methylimidazole (EMI) were purchased from Aladdin. The chemical structures of these three reactants are shown in Scheme 1. All materials were used as received without further purification.

Sample preparation

100–200 g of DGEBF and a certain amount of curing agent, D230 and DETDA, were mixed (C_{epoxy}: C_{NH} = 1: 1). Then the

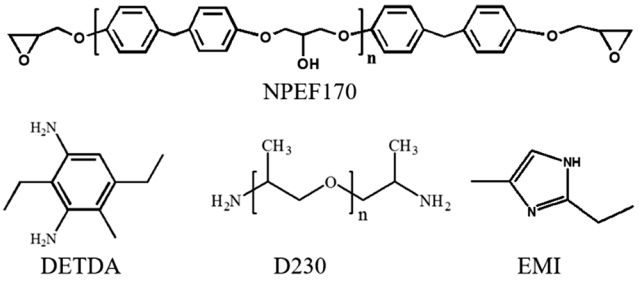

Scheme 1 Schematic presentation of the chemical structures of NPEF170, DETDA, Jeffamine D230 (n = 2.5) and EMI

mixture was mechanically stirred for 15 min before it was degassed in a vacuum oven at 60 °C for 1 h to remove air bubbles. Afterward, the degassed mixture was poured into a preheated PTFE mold and cured following the stepwise schedule: 60 °C for 2 h, 80 °C for 2 h, 130 °C for 2 h, 160 °C for 4 h, 200 °C for 4 h. The pure SMEP samples with the varying mole ratio of DETDA and D230 are denoted as T-a-D-b, where "a" and "b" are the molar contents of DETDA and D230 in the whole curing agent mixture, respectively. For example, T-20-D-80 means SMEP cured with 20% DETDA and 80% D230. Samples cured by single curing agent (D230 or DETDA) is denoted as T-0-D-100 or T-100-D-0. In addition, control samples cured with 60% DETDA and 40% D230 were prepared. Specifically, DGEBF, 60% DETDA and 40% D230 were mixed and stirred for 15 min. Then, 1 wt% EMI was mixed into the curing system and stirred for 15 min. Afterward, the degassed mixture was poured into a preheated PTFE mold and cured following the stepwise schedule: 130 °C for 3 h, 160 °C for 5 h. The control sample is denoted as S-T-60-D-40.

Characterization

Fourier transform infrared (FTIR) spectroscopy was performed on a Thermo Scientific Nicolet 6700 spectrometer in the range from 400 to 4000 cm^{-1} using KBr pellets. The differential scanning calorimetry (DSC) measurements were conducted under nitrogen using a DSC Q1000 (TA instruments) at a heating rate of 5 °C min^{-1}. The dynamic mechanical analysis (DMA) experiments were conducted in a three-point bending mode using a DMA Q800 (TA instruments). All experiments were performed in the "multifrequency, strain" mode at 1 Hz and a heating rate of 3 °C min^{-1}. The temperature where the maximum of the loss factor tan δ showed was evaluated as the (T_g). Coefficients of linear thermal expansion of different samples were measured using a TMA Q400 thermal mechanical analysis (TA instruments) in the range of 220 °C to 40 °C at a cooling rate of 2 °C min^{-1}. The specimen was made into dumbbell shaped strip (150 × 10 × 4 mm^3) and the tensile measurement of mechanical property was conducted on a universal testing machine (Instron 5567, US). Tensile measurements were conducted at room temperature and T_g of

each sample, respectively. The tensile speeds of room-temperature and high temperature are 1 mm min^{-1} and 10 mm min^{-1}, respectively. The tensile fractured surfaces of the SMEP and SMEP composites were examined by a scanning electron microscopy (SEM) instrument with an acceleration voltage of 15 kV. All the surfaces were sputtered with a thin gold film before observation. Stress relaxation test was conducted was conducted on a universal testing machine (Instron 5567, US) at T_g of each sample. The tensile strain and relaxation time were set at 10% and 30 min, respectively.

The quantitative SME analysis was conducted on a DMA Q800 (TA instruments) using force controlled mode. The heating and cooling rates were both 5 °C min^{-1}. The sample was first heated to T_g and stretched to a certain strain (3_{dload}). Subsequently, the sample was cooled to 50 °C below T_g under a constant force. Then, after equilibrium for a few minutes, the force was removed and an instantaneous recovery occurred. The strain (3_d) after this instantaneous recovery was recorded. At last, the sample was reheated to 10 °C above T_g to observe the recovery process and the final strain (3_{rec}) was recorded. Shape recovery ratio (R_r) and shape fixing ratio (R_f) were calculated according to:

$$R_r = (3_{dload} - 3_{rec}) / 3_{dload}$$

$$R_f = 3_d / 3_{dload}$$

Long-term shape fixity of each sample was tested by a separate quantitative test without DMA tester. Samples in a dog bone shape were stretched to a strain of 10% at T_g and the stretching was fixed by cooling. The deformed samples were stored at room temperature and the shape fixity was remeasured after 1 and 2 months.

The shape recovery speed of SMEP and SMEP composites were investigated by a fold-deploy shape memory test performed as follows: different rectangular samples with the dimensions of $80 \times 10 \times 1$ mm^3 were heated to T_g in an oil bath. Then The samples were bent into "V" shape. After the deformation, the samples were cooled down to a temperature 50 °C below T_g. After the shape was fixed, the bent samples were reheated to 10 °C above their T_g. The recovery process and the recovery speed were recorded by a camera and a stopwatch, respectively.

Results and discussions

Properties of SMEPs cured with single curing agents

Epoxy resins cured with different curing agents possess different network structures, which will lead to varying properties. As is shown in Fig. 1a, the tensile modulus and tensile strength of the resin cured by pure DETDA (T-100-D-0) are 2404.0 MPa and 64.7 MPa, respectively, which are much higher than that of the SMEPs cured with D230 (T-0-D-100), showing a high mechanical property. Epoxy resins cured with DETDA (T-100-D-0) also shows better thermal properties. As is shown in Fig. 2a, b, the T_g of the epoxy resin cured with pure DETDA (T-100-D-0) can be as high as 142 °C, which is 52 °C higher than that of the epoxy resins cured with D230 (T-0-D-100).

The ideal mechanical and thermal properties of T-100-D-0 are derived from the large amount of benzene rings provides the crosslinking network with more rigid and compact structure, which decreases the mobility of the molecular chains. By contrast, T-0-D-100 show inferior tensile modulus, strength and thermal performances because of the long and flexible chain of D230, resulting in a low crosslinking density of the crosslinking network.

Quantitative shape memory effect (SME) analysis was conducted on epoxy resins cured with different curing agents at varying tensile strain. The thermal–mechanical tensile curves and SME parameters are shown in Figs. 3 and 4, respectively. The SM performance of T-100-D-0 decreases severely as the strain increases. At low strain, the shape recovery ratio (R_r) and shape fixing ratio (R_f) are 89.40% and 89.32%, respectively. However, when the strain increases to 11%, the R_f and R_r decrease to 79.02% and 52.03%, respectively. On the contrary, SMEP cured with D230 (T-0-D-100) shows superior SM performances: the R_f and R_r of T-0-D-100 at low strain are 94.78% and 94.82%, respectively. Although T-0-D-100 also shows relatively poorer SM properties under a higher strain (R_f and R_r are 95.43% and 91.63%, respectively), the SM performance is much better than that of T-100-D-0, which fully reflects the contradiction between mechanical property and shape memory performance of epoxy resin.

Properties of SMEPs cured with mixed curing agents

SMEPs cured with both DETDA and D230 were prepared. An increasing dosage of D230 was added into DGEBA-DETDA system, while maintaining stoichiometry between the amine and epoxide functionalities. Generally, flexible curing agent will lead to a decrease in modulus and strength but improve the tensile elongation. Interestingly, however, we can see that a moderate dosage of D230 will not only improve the tensile elongation but also enhance both modulus and strength. As is shown in Fig. 1a, the tensile moduli of T-60-D-40 and T-80-D-20 are 2547.6 MPa and 2471.9 MPa, respectively, which are higher than that of the epoxy resin cured with pure DETDA (T-100-D-0). Meanwhile, the tensile strengths of T-60-D-40 and T-80-D-20 are 66.6 MPa and 70.9 MPa, respectively, which are 2.8% and 10.8% higher than that of the epoxy resin cured with pure DETDA (T-100-D-0). As the proportion of D230 furtherly increases, the tensile modulus and tensile strength decrease stepwise.

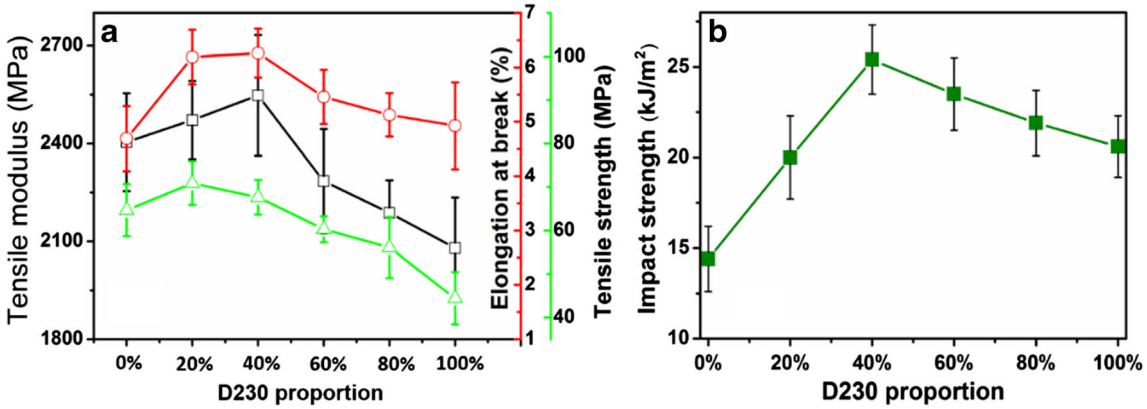

Fig. 1 Mechanical properties of SMEPs with varying ratio of D230 and DETDA: tensile modulus, tensile strength, elongation at break (**a**) and impact strength (**b**)

The elongations of the samples show similar tendency: the sample with 40% D230 proportion (T-60-D-40) instead of the sample cured with pure D230 (T-0-D-100), which possesses the most ductile structure, shows the maximum value of elongation. Furthermore, T-60-D-40 also possesses the greatest impact strength (Fig. 1b), which is 78% and 25% higher than that of T-100-D-0 and T-0-D-100, respectively. The tensile fracture surfaces of the SMEP are show in Fig. 5. The sample cured with pure DETDA shows a smooth glassy fracture surface (Fig. 5a), which indicates brittle fracture of the epoxy resin. However, the fracture surface of T-0-D-100 shows some rougher fracture sections with river-shaped lines (Fig. 5c), which is a characteristic of ductile fracture, because of the higher flexibility of D230 compared with DETDA. For samples cured with mixed curing agent (Fig. 5b), a large amount of river-shaped lines, crazings, and a much rougher fracture surface can be observed, which reflect the improved toughness of the epoxy resin cured with mixed curing agent. These results indicate that a moderate proportion of D230 will improve the toughness and strength of the epoxy resins at the same time, which is vital for a robust SMEP to achieve ideal recoverable deformation.

The SME parameters of SMEPs with varying D230 contents are summarized in Fig. 4. For simplicity's sake, only thermal–mechanical tensile curves of T-60-D-40 is selected and shown in Fig. 3. As the proportion of D230 increases, the R_f and R_r of the samples are enhanced significantly, especially at high strain. For example, the R_f and R_r of T-60-D-40 at strain of 11% are 95.01% and 89.74%, respectively, which is very close to that of T-0-D-100. Long term shape fixity measurement was conducted and results are shown in Fig.S1 (supplementary material). When D230 content is higher than 20%, shape fixity of each sample barely changes after storage for 2 months. However, for T-100-D-0 and T-80-D-20, shape fixity decreases as the storage time increases. The shape memory process and shape recovery time of SMEPs with varying D230 proportion are shown in Fig. 6. Different rectangular samples were heated to corresponding glass-transition temperature and bended into "V" shape. Then the samples were heated to 10 °C above the glass-transition temperature and the photographs were taken during the shape recovery process. As is shown, the shape recovery becomes faster as the content of D230 increases. It takes 16 s and 24 s for T-0-D-100 and T-100-D-0 to recover to the original shape, respectively. Notably, the recovery speed of T-60-D-40 is almost the same

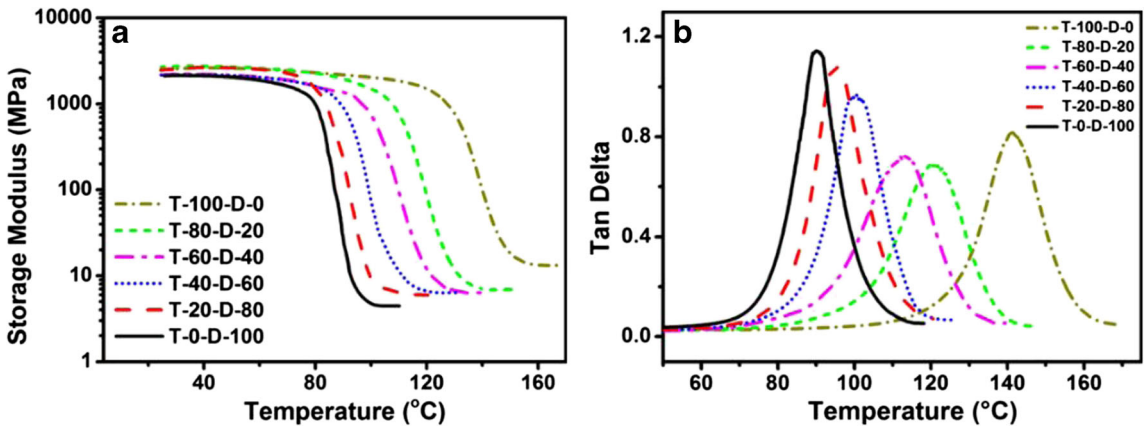

Fig. 2 DMTA curves showing the storage modulus (**a**) and tanδ (**b**) during heating of SMEP with varying DETDA proportion

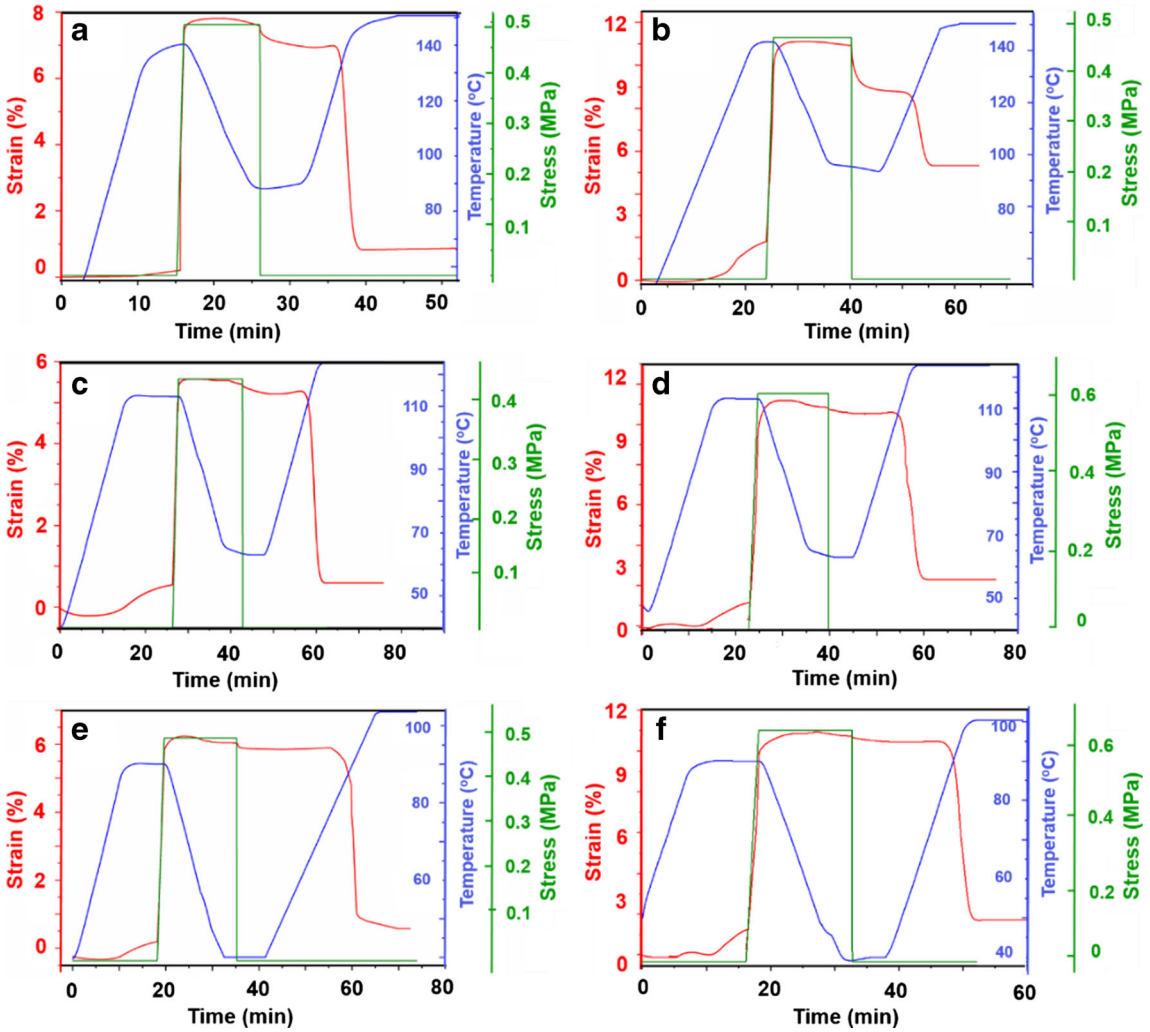

Fig. 3 The thermal–mechanical tensile curves of samples with varying ratio of D230 and DETDA at varying strains: curves of T-100-D-0 at strains of 6% (**a**) and 11% (**b**), curves of T-60-D-40 at strains of 6% (**c**) and 11% (**d**), curves of T-0-D-100 at strains of 6% (**e**) and 11% (**f**)

as that of the T-0-D-100, which is consistent with the results of the quantitative SME analysis.

Characterization of network structures

Formation of the crosslinking network

Figure 7a gives the FTIR spectra of the SMEP with varying proportion of D230. For the sake of simplicity, only three samples' FTIR spectra are given. As is shown, for each sample there is no characteristic stretching absorption peak of the epoxy group (C − O) emerging at 915 cm^{-1}. This result demonstrates that all the epoxy groups in DGEBF have been consumed during the curing reaction. The curing process was studied by DSC. As is shown in Fig. 7b, since the reactive activation energy of D230 is lower than that of DETDA, the temperature where the exothermic peak shows up decreases as the proportion of D230 increases. It is worth noting that for the

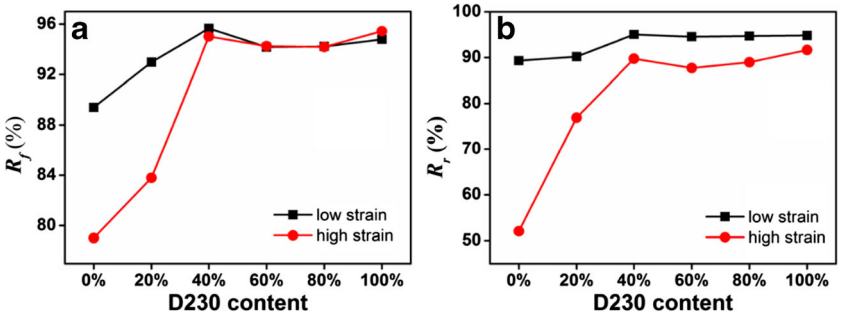

Fig. 4 R_f (**a**) and R_r (**b**) of samples cured with varying proportion of D230

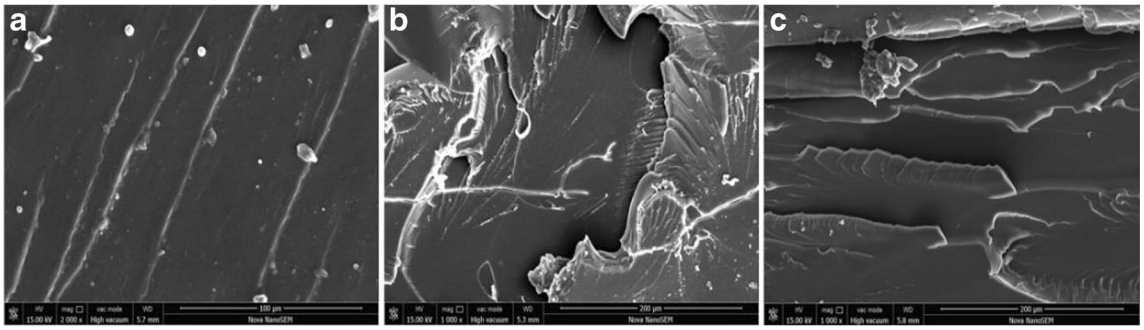

Fig. 5 SEM photographs of the tensile fractured surfaces of (**a**) T-100-D-0 (**b**) T-60-D-40 (**c**) T-0-D-100

samples of T-80-D-20, T-60-D-40 and T-40-D-60 two obvious peaks appear as the temperature increases. This is due to the difference in the reactivity of DETDA and D230. For T-80-D-20, T-60-D-40 and T-40-D-60, a fraction of epoxy groups reacted with the D230 at lower temperature in the first place because of the higher reactivity of D230. As the temperature increases, the residual epoxy groups were consumed by DETDA and the reaction heat released resulted in the emergence of the second exothermic peak. What is more, the peak derived from the exothermic reaction of the epoxy and DETDA, seems to shift leftward compared with the peak of T-100-D-0. In other words, the temperature at which the reaction between epoxy and DETDA begins decreases in the presence of D230. The phenomena may be attributed to an acceleration effect of the tertiary amine which is produced by the reaction of epoxy and D230 taking place at the first curing stage [23]. According to Andrew T. Detwiler, the successive crosslinking reaction of the epoxy with two kinds of crosslinking agent leads to two reaction stages and thus double network (DN) structures forms [24]. As is shown in Scheme 2, during the formation of the DN structure, D230 reacts firstly with the epoxy at the low temperature stage and a network with relatively low crosslinking density forms. As the temperature rises, the residual epoxy groups, including those at the end of the chains in the first network, those at the end of the free short chains and those on the unreacted DGEBF, start to react with the amino groups on DETDA and a second network forms. DSC peak fitting curves of each sample with mixed curing agents are shown in Fig. 7c-f. The theoretical fraction values of epoxy groups reacted in the first and second stage are calculated as:

$$f_1 = S_1/S_{T\text{-}0\text{-}D\text{-}100}$$
$$f_{2=}S_2/S_{T\text{-}100\text{-}D\text{-}0}$$

where S_1 and S_2 are the DSC peak areas in the first (red curve) and second (blue curve) reaction stage; $S_{T\text{-}0\text{-}D\text{-}100}$ and $S_{T\text{-}100\text{-}D\text{-}0}$ are the DSC peak areas of T-0-D-100 and T-100-D-0. The values of f_1 and f_2 are shown in Table 1. As is shown, the ratio between f_1 and f_2 is proportional to the ratio between D230 and DETDA, indicating that the first and second reaction stages are relatively independent. It is necessary to be pointed out that this model is a simplified one. Considering the secondary amine in D230 and DETDA, the curing model can be complicated. In fact, there are four stages of reaction among the epoxy group and primary amine in D230, secondary amine in D230, primary amine in DETDA, secondary amine in DETDA. When one kind of curing agent is much more than the other, the simplified model fits the DSC curve quite well. However, when the ratio of DETDA and D230 is close to 1:1,

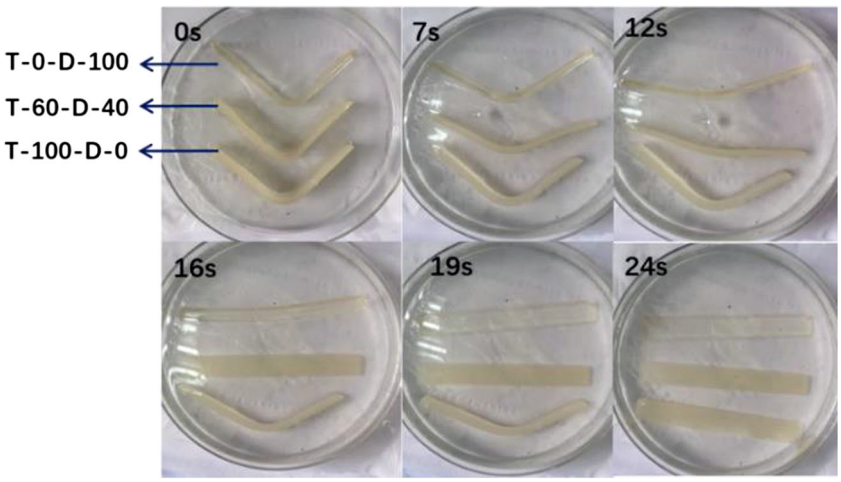

Fig. 6 The shape recovery process of SMEPs with varying DETDA proportion

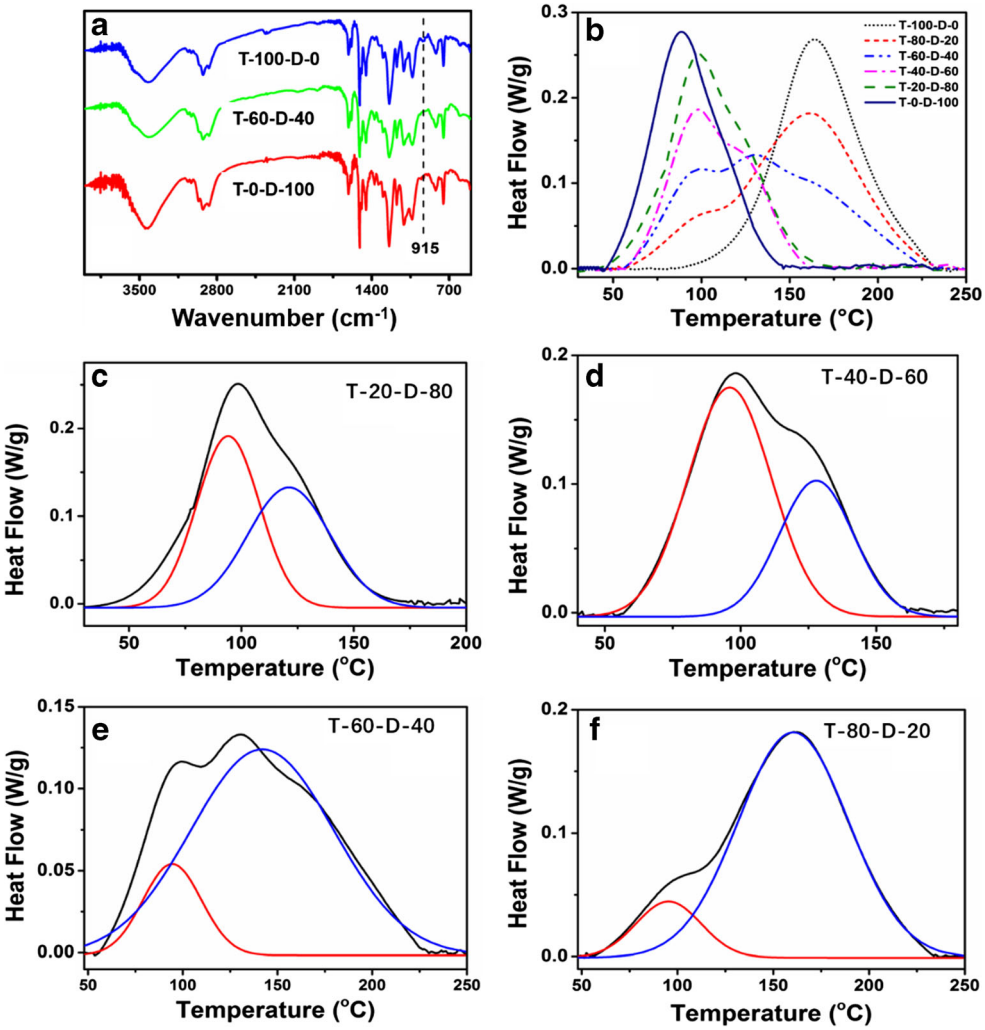

Fig. 7 FTIR spectra (**a**) and DSC thermographs (**b**) showing heat flow during heating of SMEP with varying loading of D230 (**c**-**f**) DSC peak fitting curves of each sample with mixed curing agents

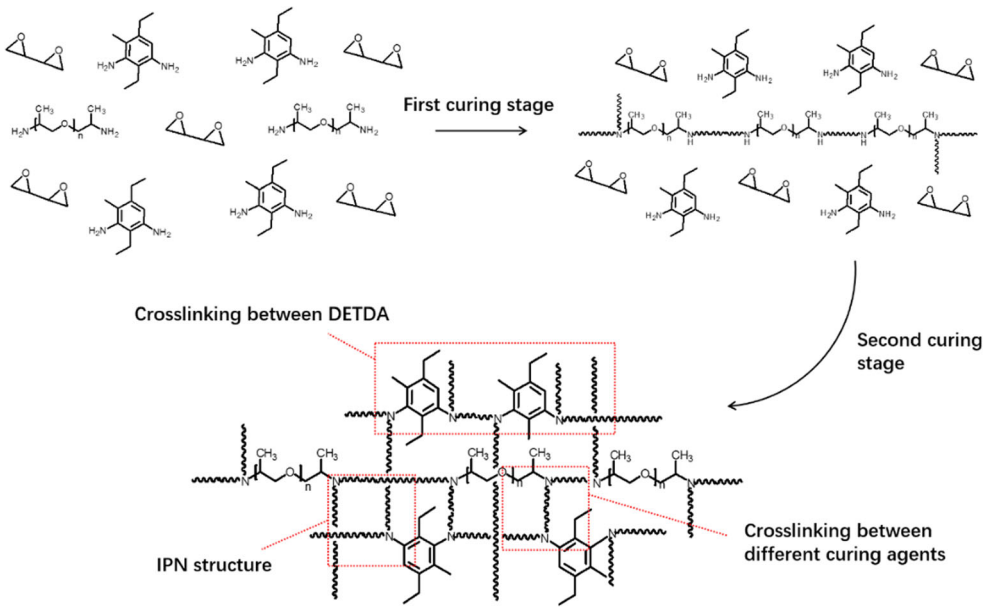

Scheme 2 Schematic diagram of the formation of the DN structure

Table 1 Results of DSC peak fitting of samples with varying D230 contents

Sample	f_1	f_2
T-20-D-80	0.73	0.18
T-40-D-60	0.53	0.36
T-60-D-40	0.26	0.72
T-80-D-20	0.15	0.83

the reactivity difference between different primary and secondary amines can not be ignored. As a result, in the case of T-60-D-40, one can see 3 peaks and obvious deviation between the fitting and experimental curves. This result is due to the fact that this simplified model is no longer applicable for this four-stage reaction system.

Dynamic mechanical analysis

DMA test was conducted to investigate network structures of different samples. In Fig. 2a, b, we can see that for each sample, only one peak of tanδ appears, which means there is no phase separation even though two crosslinking networks have formed successively during the curing process. Crosslinking densities of samples are studied by the DMA results. From the classical theory of rubber elasticity, apparent crosslinking density of each sample can be calculated from the following equation [25]:

$$v_e = \frac{E_r}{3\mathrm{RT}}$$

where E_r is the rubbery storage modulus taken 20 °C above T_g, R is the universal gas constant (8.314 J K^{-1} mol^{-1}), and T is the temperature at which the storage modulus is measured. As is shown in Table 2, as the proportion of D230 increases, the apparent crosslinking density decreases stepwise because of the longer molecular chain of D230 than that of the DETDA. Meanwhile, the storage modulus below T_g decreases stepwise as the proportion of D230 increases, suggesting the decreasing restriction of short-range molecular motions [26, 27]. It is worth noting that a sharp decrease of the apparent crosslinking density shows up as the proportion of D230 increases from 0% to 20%, while as the proportion of D230 increases furtherly the apparent crosslinking density decreases gradually. This is probably because the integrity of the rigid crosslinking network is damaged by the addition of D230, which leads to an abrupt decrease of crosslinking density. According to N. Tian [28], the structure of the amine-cured epoxy system is composed of numerous gelled clusters of higher crosslinking density. These clusters are connected at the boundary, where the crosslinking density is relatively low, forming the final network. Because of the higher reactivity, most of the D230 molecules participated in the formation of the clusters rather than the connection between clusters, which has more negative influence on the overall crosslinking density of the crosslinking network.

Table 2 Parameters of EP networks summarized and calculated from DMA

sample	T_g (°C)	Peak FWHM (°C)	E_r (MPa)	$v_e \times 10^{-3}$ (mol/cm^3)
T-100-D-0	142.2	17.8	13.1	1.20
T-80-D-20	119.5	20.6	6.9	0.70
T-60-D-40	112.3	22.6	6.7	0.69
T-40-D-60	100.6	16.4	6.3	0.67
T-20-D-80	94.8	15.3	5.9	0.64
T-0-D-100	90.1	13.4	4.3	0.47

The network homogeneity is reflected by the breadth of the tanδ peak [29, 30]. Full width at half maximum (FWHM) for the glass transitions of samples with varying D230 proportions are displayed in Table 2. As shown, the maximum value of FWHM is observed for the T-60-D-40, exhibiting the greatest heterogeneity. According to Bair HE [31, 32], the glass transition is caused by the cooperative motions of at least 10–20 atoms in the molecular chains. When epoxy resin is cured with two different kinds of curing agents, different combinations of topological connectivity will cause a higher heterogeneity of the network structure [33]. During the curing process, the aliphatic amine components all react in the first stage, forming large clusters of aliphatic amine-rich regions, while DETDA and DGEBF still remain unreacted. In the second stage, the aromatic amine reacts with the residual DGEBF. In this process, some aromatic amine-rich clusters will chemically connect with those aliphatic-rich clusters, resulting in different combinations of topology connectivity. Meanwhile, some amine-rich clusters permeate those aliphatic amine-rich clusters, leading to the formation of a local IPN or semi-IPN structure, in which large amounts of interpenetration among polymer chains or gelled clusters exist (as shown in Scheme 2). The difference in the combinations of topology connectivity and interpenetration both contribute to the increased heterogeneity of the network [24]. When the molar ratio of DETDA to D230 is close to 1:1, approximately equal amount of DGEFF is consumed during the formation of the DN structure, ensuring the integrity of the first and second network. Thus, T-60-D-40 and T-40-D-60 show much higher heterogeneity than any other samples because of the highest degree of topological variety.

Thermomechanical analysis

According to X. Miao et al. [34–36], the fractional free volume (f_T) can be expressed as $f_T = f_g + \Delta\alpha$ (T-T_g), where $\Delta\alpha$ is the difference between the volumetric coefficients of thermal expansion (CTE) in the rubbery and glassy states,

respectively, and f_g is the fractional free volume "frozen" at T_g. Thus, $\Delta\alpha$ is directly proportional to fractional free volume [37]. Results of TMA test are shown in Table 3. $\Delta\alpha$ of T-0-D-100 is much higher than that of T-100-D-0, while $\Delta\alpha$ of samples cured with mixed curing agents is much higher than that of T-0-D-100, indicating that samples cured with mixed curing agents have higher fractional free volume than that cured with single curing agent. The fractional free volume is affected by both crosslinking density and network structure. The lower crosslinking density of T-0-D-100 leads to a relatively loose network, which creates a much higher free volume than that of T-100-D-0. As for samples cured with mixed curing agents, though the crosslinking density are higher than that of T-0-D-100, fractional free volume still increases because of the physical network, where interpenetrations produce larger volume than chemical crosslinking do. T-60-D-40 shows the highest value of $\Delta\alpha$, indicating the highest fractional free volume, because the molar ratio of DETDA to D230 is close to 1:1, ensuring the integrity of the first and second network.

Stress relaxation test

As shown in Fig. 8, the almost "ideal elastic" network of T-0-D-100 shows very small viscoelastic effect. In contrast, samples cured with mixed curing agents show significant viscoelastic effects. Stress relaxation test was also conducted for S-T-60-D-40. As is mentioned above, the successive crosslinking reaction of the epoxy with two kinds of crosslinking agent will leads to DN structure. However, for S-T-60-D-40, D230 and DETDA participate in the reaction almost simultaneously because of the acceleration effect of EMI. Thus, only one exothermic peak shows up as the temperature increases (supplementary material Fig. S2), indicating that a single network structure forms in S-T-60-D-40. As shown in Fig. S3 (supplementary material), S-T-60-D-40 exhibits slight viscoelastic effect, while T-60-D-40 exhibits obvious relaxation effect. For this reason, the significant difference in viscoelastic behavior is believed to be caused by the dissociation of the physical network in the T-60-D-40 crosslinking network. The viscoelastic behavior and

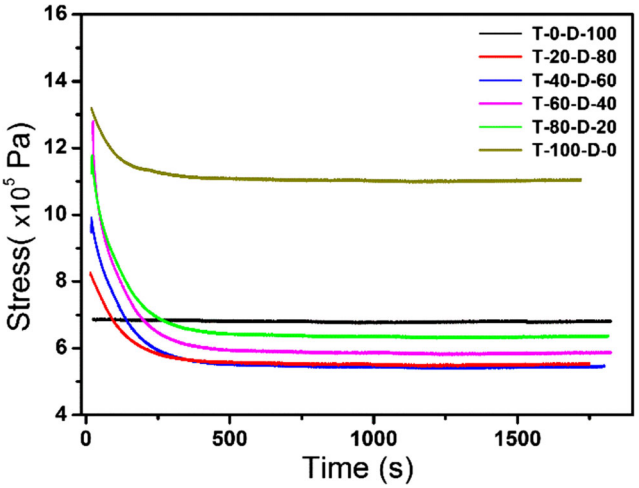

Fig. 8 Stress relaxation curves of SMEPs with varying D230 proportion

relaxation of samples with varying D230 proportion are characterized in Table 4. For simplicity, the viscoelasticity effect is expressed as $\Delta\sigma_{VE} = (\sigma_0 - \sigma_e)/\sigma_0$, where σ_0 and σ_e are the initial (at $t = 0$) and equilibrium stress at deformation, respectively, while T_{relax} refers to the time of relaxation up to equilibrium of stress. As is shown, when the D230 proportion was 40% (T-60-D-40), $\Delta\sigma_{VE}$ and T_{relax} reach the maximum value, 0.55 and 9.6 min, respectively. For T-60-D-40, the greatest viscoelastic behavior indicates the maximum integrity of the physical network is achieved, which is consistent with the result of DMA and TMA. Under this condition, when samples are subjected to tension loading, breaking of the physical network will happen before the breakage of chemical bond.

Relationship between network structures and properties

As the proportion of D230 increases, all the mechanical property parameters of SMEPs, including tensile modulus, tensile strength and elongation at break, show the same trend: first increase and then decrease. When the proportion of D230 increases to 40%, the SMEP shows the highest strength and toughness. It can be deduced that it is the DN structure that brings about enhanced mechanical performances. As is discussed above, the maximum value of FWHM is observed

Table 3 Linear coefficients of thermal expansion of different samples

sample	α_g ($\times 10^6$ K^{-1})	α_r ($\times 10^6$ K^{-1})	$\Delta\alpha$ ($\times 10^6$ K^{-1})
T-100-D-0	76.0	213.7	137.7
T-80-D-20	73.1	215.9	142.8
T-60-D-40	69.8	229.7	159.9
T-40-D-60	62.4	218.4	156.0
T-20-D-80	56.6	210.0	153.4
T-0-D-100	50.2	201.3	151.1

Table 4 The viscoelastic behavior and relaxation of SMEPs

sample	T_{relax} (min)	$\Delta\delta_{VE}$
T-100-D-0	4.5	0.13
T-80-D-20	8.3	0.45
T-60-D-40	9.6	0.55
T-40-D-60	5.6	0.42
T-20-D-80	5.	0.32
T-0-D-100	0	0

for the T-60-D-40, exhibiting the greatest heterogeneity. On the other hand, the FWHM also reflects the network's ability to dissipate energy [37, 38]. The physical network in the DN network leads to higher energy dissipation and higher free volume, which can endow the sample with higher toughness.

On the other hand, physical network in the DN structure also makes contribution to the strength of the network. To better investigate the effect of DN structure on the mechanical strength, high-temperature tensile test was conducted at each sample's T_g. As is shown in Fig. 9, T-100-D-0 shows the poorest elongation of 20.8% because of the higher crosslinking density of the rigid network. As for the samples cured with mixed cured agents, the elongation increases significantly because of the reduced crosslinking density and larger space for configuration adjustment. When the proportion of D230 reaches 40% instead of 100%, the elongation of the sample shows the highest value (47.8%). What is more, the stress of T-60-D-40 is 3.75 MPa, which is the highest value among all the samples. Under tensile strength, when the interpenetrating chains get to an extreme, the tense chains will provide strength for the network. That is why T-60-D-40, which possesses high integrity of the first and second network, shows the highest strength and modulus either at room temperature or at T_g. The reinforcing effect of the DN structure is more significant when compared with chemical crosslinking systems along with physical entanglements. For example, in the work of A.B. Leonardi et al. [39], an SMEP with pendant alkyl chains undergoing tail-to-tail entanglement was designed to improve the shape memory property. When stretched to a strain of 45% at T_g, the stress was 2.4 Mpa, which was much lower than that of T-60-D-40 (3.75 MPa).

The SM performance of a SMEP is determined by the network structure. The poor R_f and R_r of T-100-D-0, especially at a relatively high strain, can be correlated to the high crosslinking density and stiffness of the network, which are revealed by the high value of v_e and low elongation at the deformation temperature. As is shown in Fig. 9, the maximum tensile strain of T-100-D-0 at T_g is 20%. When the tensile strain increased to 10%, the large deformation causes irreversible structure changes (which results in the fast decrease of the stress in the stress relaxation test), leading to a low R_r. Meanwhile, the high modulus of the sample in rubber state results in a low R_f. On the contrary, it is easy for SMEP with a flexible network to fix and recover shape because of the high elongation and low modulus at the deformation temperature. That is why T-0-D-100 shows the highest R_f and R_r. Whereas for samples cured with mixed curing agents, for example, T-60-D-40, a higher elongation at the deformation temperature and a longer relaxation time (Fig. 8 and Fig. 9) are both in favor of shape fixity and shape recovery. During the tensile process in the SM test, the stress is removed before the breaking of the physical network, leading to only short-range deformation of the network, which is easy to be fixed and recover. Also, the tensile strain in the SM test (11%) is much lower than the extreme elongation at the deformation temperature (47.8%). Thus, R_f and R_r of T-60-D-40 still maintained at a high level. Similarly, the rigid network structure and higher crosslinking density of T-100-D-0 bring about a much larger steric hindrance during the recovery process, which means it will take more time for the molecular chains to recover to its original state to release entropy, while T-60-D-40 and T-0-D-100 have much faster recovery speed owing to the ductile crosslinking network and improved toughness. Though the existence of DETDA still impairs the recovery speed to some extent, a proper ratio of DETDA and D230 can guarantee an ideal recovery speed owing to the adjustability of the physical network in the DN structure.

Conclusion

To solve the contradiction between high strength mechanical properties and ideal shape memory performances, shape memory epoxy resins(SMEPs) with both high mechanical property and ideal shape memory performances were prepared by constructing double network structure through employing two kinds of curing agents with different reactivity.: poly(propylene glycol)bis(2-aminopropyl) ether(D230) and diethyltoluenediamine (DETDA). When the proportions of D230 is 40%, tensile modulus at room temperature reaches

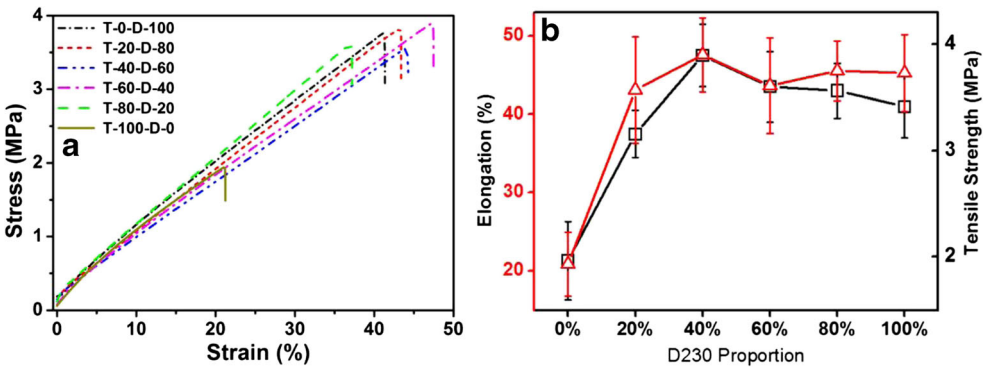

Fig. 9 High-temperature tensile curves (**a**) and tensile strength and elongation (**b**) of SMEPs with varying D230 proportion

2547.6 MPa, tensile stress reaches 66.6 MPa and strain at break is above 6%, which are all enhanced compared with that of the sample cured with single curing agent. The shape memory test shows that the shape fixing ratio, shape recovery ratio and shape recovery speed still maintain at an ideal level when the proportion of D230 is 40%, while sample cured with pure DETDA shows inferior shape memory property, especially at high tensile strain, because of the steric hindrance and immobilization effect. DSC results show that the formation of network of sample cured with mixed curing agents can be divided into two steps because of the different reactivity of the curing agents, which may lead to a unique double network structure. The double network structure was characterized by DMA, TMA, and stress relaxation tests. It is found that the physical network in the double network structure can improve the strength and toughness simultaneously. Meanwhile, the increased elongation and low modulus in rubbery state endow the SMEPs with ideal shape memory properties. All these results show that an appropriate amount of D230 will lead to a DN network structure which can enhance the mechanical property of epoxy resin without compromising the shape memory property. This finding may provide a new perspective for preparing high performance shape memory epoxies.

Acknowledgements This work was supported by the State Key Scientific Special Project (2016ZX05017-002) of China.

References

1. Alteheld A, Feng Y, Kelch S, Lendlein A (2002) Biodegradable, amorphous copolyester-urethane networks having shape-memory properties. Angew Chem Int Ed 41:2034–2057
2. Behl M, Razzaq MY, Lendlein A (2010) Multifunctional shape-memory polymers. Adv Mater 22:3388–3410
3. Liu C, Qin H, Mather PT (2007) Review of progress in shape-memory polymers. J Mater Chem 17:1543–1558
4. Liu Y, Han C, Tan H, Xingwen D (2010) Thermal, mechanical and shape memory properties of shape memory epoxy resin. Mater Sci Eng A 527:2510–2514
5. Rousseau IA (2008) Challenges of shape memory polymers: a review of the progress toward overcoming SMP's limitations. Polym Eng Sci 48:2075–2089
6. Gunes IS, Jana SC (2008) Shape memory polymers and their nanocomposites: a review of science and technology of new multifunctional materials. J Nanosci Nanotechnol 8:1616–1637
7. Ge Q, Luo X, Iversen CB, Mather PT, Dunn ML, Qi HJ (2013) Mechanisms of triple-shape polymeric composites due to dual thermal transitions. Soft Matter 9:2212–2223
8. Qi X, Guo Y, Wei Y, Dong P, Qiang F (2016) Multishape and temperature memory effects by strong physical confinement in poly(propylene carbonate)/graphene oxide nanocomposites. J Phys Chem B 120:11064–11073
9. Lendlein A (2010) Progress in actively moving polymers. J Mater Chem 20:3332–3334
10. Bai Y, Chen Y, Wang Q, Wang T (2014) Poly(vinyl butyral) based polymer networks with dual-responsive shape memory and self-healing Properties. J Mater Chem A 2:9169–9177
11. Zhang RR, Guo XG, Liu YJ, Leng JS (2014) Theoretical analysis and experiments of a space deployable truss structure. Compos Struct 112:226–230
12. Kang HL, Li MQ, Tang ZH, Xue JJ, Hu XR, Zhang LQ, Guo BC (2014) Synthesis and characterization of biobased isosorbide-containing copolyesters as shape memory polymers for biomedical applications. J Mater Chem B 2:7877–7886
13. Liu Y, Zhao J, Zhao L, Li W, Zhang H, Yu X, Zhang Z (2016) High performance shape memory epoxy/carbon nanotube nanocomposites. ACS Appl Mater Interfaces 8:311–320
14. Ponyrko S, Donato RK, Matějka L (2016) Tailored high performance shape memory epoxy–silica nanocomposites. Structure design. Polym Chem 7:560–572
15. Zheng N, Fang G, Cao Z, Zhao Q, Xie T (2015) High strain epoxy shape memory polymer. Polym Chem 6:3046–3053
16. Xie T, Rousseau IA (2009) Facile tailoring of thermal transition temperatures of epoxy shape memory polymers. Polymer 50: 1852–1856
17. Ohki T, Ni QQ, Ohsako N, Iwamoto M (2004) Mechanical and shape memory behavior of composites with shape memory polyme. Compos A: Appl Sci Manuf 35:1065–1073
18. Jung YC, Sahoo NG, Cho JW (2006) Polymeric nanocomposites of polyurethane block copolymers and functionalized multi-walled carbon nanotubes as crosslinkers. Macromol Rapid Commun 27: 126–131
19. Liu T, Nie Y, Zhang L, Chen R, Meng Y, Li X (2015) Dependence of epoxy toughness on the backbone structure of hyperbranched polyether modifiers. RSC Adv 5:3408–3416
20. Nakajima T, Furukawa H, Tanaka Y, Kurokawa T, Osada Y, Gong JP (2009) True chemical structure of double network hydrogels. Macromolecules 42:2184–2189
21. Singh NK, Lesser AJ (2011) A physical and mechanical study of prestressed competitive double network thermoplastic elastomers. Macromolecules 44:1480–1490
22. Thiele JL, Cohen RE (1979) Synthesis, characterization and viscoelastic behavior of single-phase interpenetrating polystyrene networks. Polym Eng Sci 19:284–293
23. Smith IT (1961) The mechanism of the crosslinking of epoxide resins by amines. Polymer 2:95–108
24. Detwiler AT, Lesser AJ (2012) Characterization of double network epoxies with tunable compositions. J Mater Sci 47:3493–3503
25. Flory PJ (1979) Molecular theory of rubber elasticity. Polymer 20: 1317–1320
26. Tu J, Tucker SJ, Christensen S, Sayed AR, Jarrett WL, Wiggins JS (2015) Phenylene ring motions in isomeric glassy epoxy networks and their contributions to thermal and mechanical properties. Macromolecules 48:1748–1758
27. Marks MJ, Snelgrove RV (2009) Effect of conversion on the structure− property relationships of amine-cured epoxy thermosets. ACS Appl Mater Interfaces 1:921–926
28. Tian N, Ning R, Kong J (2016) Self-toughening of epoxy resin through controlling topology of cross-linked networks. Polymer 99:376–385
29. Miao X, Meng Y, Li X (2015) A novel all-purpose epoxy-terminated hyperbranched polyether sulphone toughener for an epoxy/amine system. Polymer 60:88–95
30. Cook WD, Scott TF, Quay-Thevenon S, Forsythe JS (2004) Dynamic mechanical thermal analysis of thermally stable and thermally reactive network polymers. J Appl Polym Sci 93: 1348–1359
31. Boyer RF (1963) The relation of transition temperatures to chemical structure in high polymers. Rubber Chem Technol 36:1303–1421
32. Hale A, Macosko CW, Bair HE (1991) Glass transition temperature as a function of conversion in thermosetting polymers. Macromolecules 24:2610–2621

33. Beck Tan NC, Bauer BJ, Plestil J, Barnes JD, Liu D, Matejka L (1999) Network structure of bimodal epoxies—a small angle X-ray scattering study. Polymer 40:4603–4614
34. Lv J, Meng Y, He L, Qiu T, Li X, Wang H (2013) Novel epoxidized hyperbranched poly (phenylene oxide): synthesis and application as a modifier for diglycidyl ether of bisphenol A. J Appl Polym Sci 128:907–914
35. Luo L, Meng Y, Qiu T, Li Z, Yang J, Cao X, Li X (2013) Dielectric and mechanical properties of diglycidyl ether of bisphenol a modified by a new fluoro-terminated hyperbranched poly (phenylene oxide). Polym Compos 34:1051–1060
36. Strobl G (2007) The physics of polymers: concepts for understanding their structures and behavior. In: The semicrystalline state, pp 165–222
37. Ratna D, Simon GP (2010) Epoxy and hyperbranched polymer blends: Morphology and free volume. J Appl Polym Sci 117:557–564
38. Wu WL, Hu JT, Hunston DL (1990) Structural heterogeneity in epoxies. Polym Eng Sci 30:835–840
39. Leonardi AB, Fasce LA, Zucchi IA, Hoppe CE, Soulé ER, Pérez CJ, Williams RJJ (2011) Shape memory epoxies based on networks with chemical and physical crosslinks. Eur Polym J 47:362–336